

# NJC

Accepted Manuscript



This is an *Accepted Manuscript*, which has been through the Royal Society of Chemistry peer review process and has been accepted for publication.

*Accepted Manuscripts* are published online shortly after acceptance, before technical editing, formatting and proof reading. Using this free service, authors can make their results available to the community, in citable form, before we publish the edited article. We will replace this *Accepted Manuscript* with the edited and formatted *Advance Article* as soon as it is available.

You can find more information about *Accepted Manuscripts* in the [Information for Authors](#).

Please note that technical editing may introduce minor changes to the text and/or graphics, which may alter content. The journal's standard [Terms & Conditions](#) and the [Ethical guidelines](#) still apply. In no event shall the Royal Society of Chemistry be held responsible for any errors or omissions in this *Accepted Manuscript* or any consequences arising from the use of any information it contains.

## ARTICLE

## Dissolution and Reduction of Cobalt ions in Polyol Process Using Ethylene Glycol - Identification of the Active Species and its Role -

Cite this: DOI: 10.1039/x0xx00000x

Received 00th January 2012,  
Accepted 00th January 2012

DOI: 10.1039/x0xx00000x

[www.rsc.org/](http://www.rsc.org/)Takatoshi Matsumoto,<sup>a</sup> Kazuma Takahashi,<sup>b</sup> Keisuke Kitagishi,<sup>b</sup> Kozo Shinoda,<sup>a</sup> Jhon. L. Cuya Huaman,<sup>b</sup> Jean. Y. Piquemal,<sup>a</sup> and Balachandran Jeyadevan<sup>\*b</sup>

Polyol process has been used to synthesize metal and alloy nanoparticles over decades. However, though the role of polyol has been identified as a reducing agent, the details have not been clarified fully. In this manuscript, determination of the active polyol species and its role in the synthesis of metal nanoparticles has been attempted both experimentally and theoretically using the ethylene glycol (EG) as the medium and cobalt as the metal source. Molecular orbital calculations carried out considering dianion, monoanion and neutral states of ethylene glycol species suggested that the monoanion state of ethylene glycol is the most active form. Subsequently, this was verified experimentally using different types of cobalt salts in ethylene glycol. The cobalt salts that could dissociate easily and the deprotonation of ethylene glycol by its counter anion were vital for the progression of the dissolution and reduction reaction of cobalt ions to form cobalt metal particles. Furthermore, the acceleration of the dissolution and reduction reaction by the addition of hydroxyl ions also confirmed the deprotonation reaction of ethylene glycol. In conclusion, the experimental and theoretical studies have proved that the monoanion of ethylene glycol is the active species that not only assumes a role in the reduction of metal, but also plays an important role in the dissolution and formation of the intermediate metallic complex, which is vital for their subsequent reduction reaction.

### Introduction

In recent years, the synthesis of metal and alloy nanoparticles, nanorods, nanowires, etc. and their application in the field of nanostructure-based technology has been on the rise.<sup>1-5</sup> To cater the demand in the above fields, various solution-based techniques have been developed and utilized successfully for the synthesis of elements varying from noble to transition metals.<sup>6-27</sup> Though the thermal decomposition technique gained grounds at the initial stages, issues related safety and environmental concerns have prompted the researchers to resort to alternative techniques.<sup>28-36</sup> As a result, the use of polyol process has gained momentum and Fe and Fe-based alloys,<sup>37-42</sup> which were normally considered difficult, also have been achieved besides relatively easily reducible other transition and noble metals and their alloys.<sup>43</sup> Consequently, the potential of polyol process has widely recognized and has been extended to the synthesis of easily reducible metals using straight chained alcohols (Cu, Ni, Ag).<sup>44-46</sup> However, the control over their physical properties such as size, size distribution, and shape of the metal and alloy particles has been limited to easily reducible

metals. The reason has been due to the limited understanding of the reaction process including the dissolution of metal precursor and the reduction reaction in the polyol medium. Though some effort has been made to understand oxidation reaction of the polyol, the study has been confined to ethylene glycol.<sup>47-49</sup> And also, the contradicting behaviour of metal precursors, for example, different cobalt salts in ethylene glycol, some of which does not get reduced to form metals, is yet to be explained. Authors believe that the elucidation of the reaction mechanism in polyol process is vital not only for the designed synthesis of already demonstrated metal and alloy particles, but also for many novel nanomaterials to be produced in the future.

In this paper, we report the (a) theoretical estimation of the active species in ethylene glycol, (b) verification of the theoretically predicted active species through experiments and (c) structure identification of complexes formed in cobalt-ethylene glycol and cobalt-ethylene glycol-hydroxide systems. The identification of the active species in polyol helps us to understand the dissimilar behaviour of different cobalt metal salts and their subsequent complexation on one hand and the

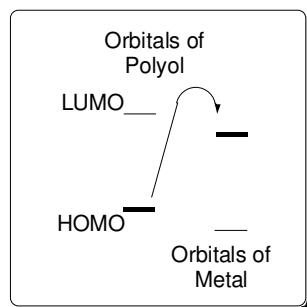


Fig. 1 Schematic diagram describing the electron transfer between polyol and metal salt.

structural transformation of the metal complexes on the other. The theoretical and experimental results have made the formulation of a unified scheme for the dissolution of the metal precursor in polyol, subsequent complexation with polyol, structural transformation through the oxidation of ethylene glycol to produce metal cobalt particles. It should be noted that results reported here are very specific to cobalt system; however, this information could be easily transferred to other transition metal precursors considering the stability of the complexes formed in such cases.

## Experimental

### Theoretical Calculation

Theoretical calculations were performed on ethylene glycol, which is one of the representative polyol used for the synthesis of transition as well as noble metals. In addition, the source for the metal nanoparticle and sodium hydroxide, which is often used as the reaction promoter, is considered. The presence/absence of sodium hydroxide holds the key in the elucidation of the reaction mechanism in polyol process. In polyol process, when nanometal particle is produced through the reduction of the metal complex, the metal compound receives electron from polyol through redox reaction. The electron transfer depends on the orbital energy possessed by the compounds. The electron in the HOMO (Highest Occupied Molecular Orbital) of polyol will be transferred to the orbital corresponding to LUMO (Lowest Unoccupied Molecular Orbital) of the metal salt as shown in Fig. 1. This electron transfer reaction progresses easily when the energy difference between the electron orbitals is small. In the quantum chemical calculations used here, the temperature effect is covered by considering the conformational changes in polyol sufficiently. Consequently, when we consider the orbital energy fixing the type of metal salt, the HOMO energy value of polyol that acts as the reducing agent becomes very important.

In polyol process, the polyol could undergo reactions with additives that might be present in the system and give rise to different electronic states of polyol. Thus, in this study, we have considered dianion (**1**), monoanion (**2**) and neutral states (**3**) as possible active forms of ethylene glycol. Subsequently, we decided to study the above three structures and their properties. The rotational dihedral angle of possible ethylene

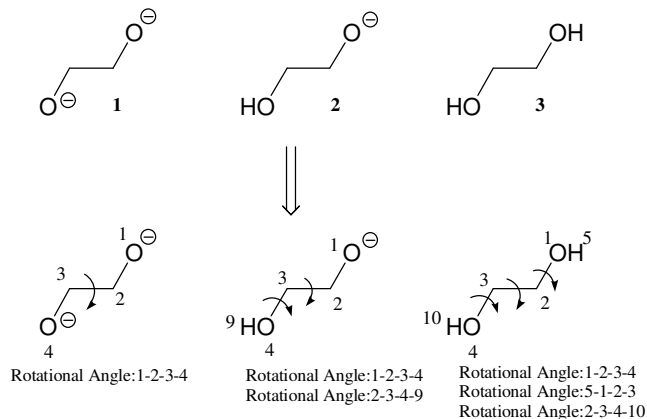


Fig. 2 Possible ethylene glycol derived species in the reaction system and their rotating dihedral angles.

glycol derived species in the reaction system is shown in Fig. 2. The 3D initial coordinates of target compounds used in the calculation were drawn using the CS Chem3D Ver. 7.0. *Ab initio* calculations were carried out using program Gaussian 98 A.11.3<sup>50</sup> on Linux PC-Cluster. LanL2MB<sup>51-55</sup> of Gaussian 98 was used for structure optimization and orbital energy calculations. The reason for the selection of the above base function was to make the comparison with metal salts including the transition metals possible. Though it was possible to reduce the amount of computation by considering the symmetry of molecular structure, the symmetry was not taken into account purposely to avoid the counting loss of conformational isomers. Berny algorithm was used for structural optimization of all initial coordinates. Furthermore, the fulfillment of the standard convergence conditions such as maximum force component, root-mean-square force, maximum displacement component, and root-mean-square displacement, are implemented during the calculations.

### Experimental Verification

**Sample Preparation:** All hydrated cobalt salts (acetate and chloride), ethylene glycol (EG), sodium metal, sodium hydroxide, dodecane and methanol were used without any further purification. The steps involved in a typical experiment are as follows: 0.01 M metal salt is dissolved in 0.1 M of ethylene glycol followed by the addition of either sodium metal or sodium hydroxide. Then, the ethylene glycol-metal salt or ethylene glycol-metal salt-sodium/sodium hydroxide system is heated to specified temperatures to obtain required by-products or cobalt metal particles. The samples are recovered by centrifuging the suspension and subsequently washed with methanol. Then, the products obtained are dried in vacuum at room temperature (R.T) prior to further analysis.

**Characterization:** UV-Vis spectrometric analysis was carried out on solution samples using the Hitachi U-3300 UV-Vis Spectrophotometer to identify the metal complexes formed during various stages of the reaction. Powder X-ray diffraction (XRD) patterns of the precipitates were carried out using the Panalytical X'pert pro diffractometer (Cu K $\alpha$  1.541 Å). The

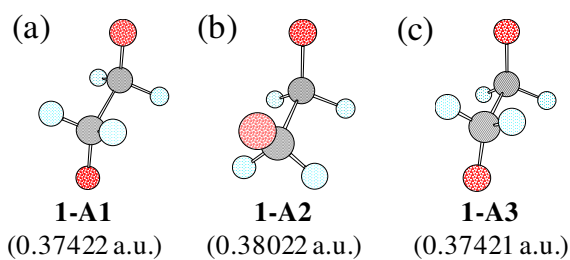


**Fig. 3** Conformers obtained from relative SCF energies for (a) 180, (b) 0 degree cases and (c) minimum HOMO energies (at 170 degrees).

local structure of the metal complexes were carried out using an in-house X-ray absorption spectrophotometer (Rigaku R-XAS Looper) housing a demountable X-ray tube with Mo target as the white X-ray source and Si(400) Johansson-type bent single crystal as the monochromator crystal. The local atomic environmental structure around a Co, the XAFS spectrum of the sample for the Co-K edge was recorded and analyzed. Morphology of the products was characterized using Hitachi-FE-SEM 4500 scanning electron microscopy using an accelerating voltage of 15 kV. The R.T magnetic data were collected using the vibration sample magnetometer (Tamagawa TM-VSM 1230-HHH5) on dried samples.

## Results and discussion

### Determination of the true active species derived from ethylene glycol

Understanding the reaction mechanism is absolutely imperative to consider the experimental conditions to have finer control over the physical properties of the metal particles produced by polyol process. Thus, for optimal nanoparticle synthesis, (a) determination of the true active species derived from ethylene glycol and (b) the optimal combination between polyol and metal salt types, are important.

However, in this study first we confine ourselves to the identification of true active species derived from ethylene glycol which is very vital in the designed synthesis of metal nanoparticles, through theoretical estimation. And then, we subsequently verify the theoretical prediction experimentally. Especially, the EG-Co case in the presence and absence of

hydroxyl ions will be considered using different cobalt metal salts to verify the theoretical predictions experimentally.

In the sections below, the theoretical estimations for dianion, monoanion and neutral states of ethylene glycol will be discussed in detail by evaluating the relative self-consistent field (SCF) energies estimated from most stable conformer and HOMO energy for each conformer.

### Dianion derived from ethylene glycol

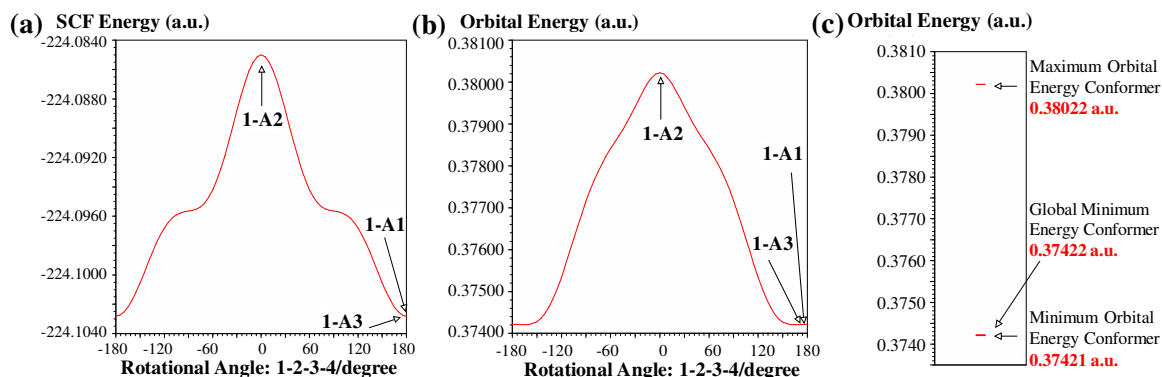
Dianion is a state where both hydrogen atoms are removed from the two hydroxyl groups in ethylene glycol. The conformers obtained from relative SCF energies for different conditions are given in Fig. 3. When the relative SCF energies estimated from most stable conformer and HOMO orbital energies of each conformer for dianion rotated at dihedral angle around O-C-C-O, the most stable conformer is observed at +180 degrees and the highest relative energy is obtained at 0 degree. The minimum relative energy is recorded when the oxygen in the anion states are farther away from each other. On the other hand, maximum energy including the high electrostatic repulsion is recorded when anion state oxygen atoms approach each other. Moreover, the lowest HOMO orbital energy is 1.13 kcal $\cdot$ mol $^{-1}$  higher than the relative SCF energy of the most stable conformer.

Furthermore, when the HOMO energies of the conformers shown in Fig. 4(a)-(b) were plotted as the 1D coordinate axes, the HOMO energies assumed discontinuous values as shown in Fig. 4(c). In other words, the fingerprint of HOMO orbital energies is specific to dianion and takes a single value other than the maximum HOMO orbital energy derived from the unstable conformer.

### Monoanion derived from ethylene glycol

Monoanion is a state where a hydrogen atom is removed from one of the two hydroxyl groups in ethylene glycol. The SCF and HOMO energy surfaces of most stable conformer was determined by rotating the monoanion around face angles O-C-C-O (rotational angle 1) and H-O-C-C (rotational angle 2) and the results are shown in Fig. 5(a) and (b), respectively (enlarged figure is given in Fig. S1). From SCF energy surface, the most

**Fig. 4** (a) SCF, (b) HOMO and (c) the fingerprint of HOMO energies of each conformation for dianion species derived from ethylene glycol.



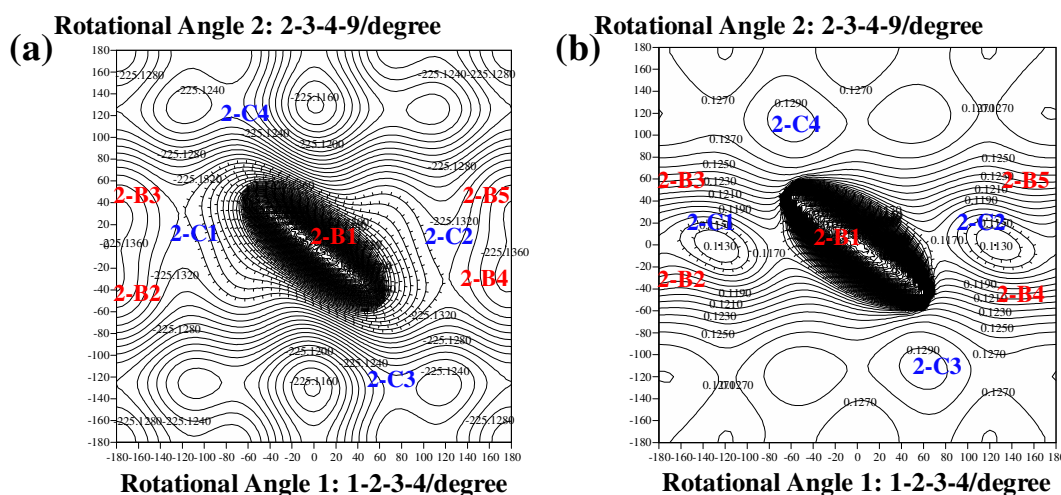


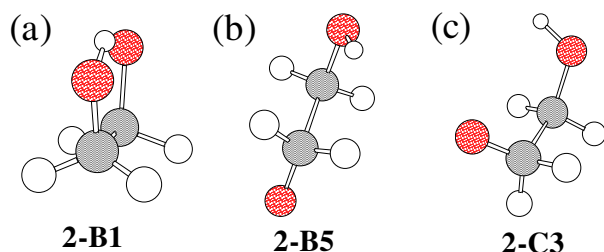
Fig. 5 (a) SCF and (b) HOMO energy surfaces at each conformer for the ethylene glycol at monoanion state.

stable conformer was determined to be **2-B1** (0 (angle 1), 0 (angle 2)). Besides the above, four other stable conformers, **2-B2** (-180,-25), **2-B3** (-175,25), **2-B4** (175,-25), and **2-B5** (180,20) exist. However, their relative SCF energies are 35.6 kcal•mol<sup>-1</sup> higher than **2-B1** conformer. The characteristic conformers of the ethylene glycol in the monoanion state are given in Fig. S2.

In the most stable conformer **2-B1**, the formation of the hydrogen bond through electrostatic attraction between the oxygen in the anion state and the hydrogen in the hydroxyl group contributes to the stability, as shown in Fig. 6(a). In all other relatively stable conformers such as **2-B2**, **2-B3**, **2-B4**, **2-B5**, the oxygen in the anion state and the hydroxyl group face opposite direction (Fig. 6(b)) and the hydrogen bond that contributes to the stabilization of the conformer cannot be formed. On the other hand, in the cases of **2-C1** and **2-C2** derived from the HOMO energy surface as shown in Fig. 5(b), the hydrogen in the carbon bond that corresponds to the base of the oxygen in the anion state and hydroxyl group in the opposite side confront with each other. This results in a weak steric repulsion and the relative SCF energy difference from the stable conformers except for **2-B1**, becomes 2.2 kcal•mol<sup>-1</sup> higher and leads to destabilization.

Furthermore, **2-C3** (60,-110) (Fig. 6c) and **2-C4** (-60,110) (refer Fig. S2) had the highest HOMO energy (0.12943 a.u.)

Fig. 6 Characteristic conformers of the mono-anion state derived from ethylene glycol.

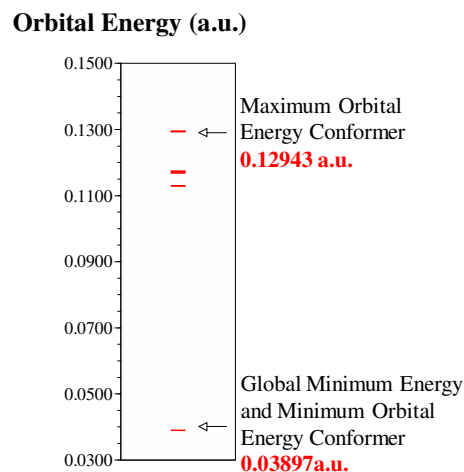


and appeared on the slope as shown in Fig. 5(a). The HOMO energies of conformer obtained from the relative SCF energy surface and the HOMO energy surface in Fig. 5(a) and (b) were plotted in 1D coordinate axis as shown in Fig. 7. Even in the monoanion state, HOMO energies take discrete values. The energy difference between **2-B1** that possesses lower most energy and second lowest HOMO energy conformer **2-B5** (0.11684 a.u.) is 2.12 eV.

#### Neutral state of ethylene glycol

As shown in Fig. 2, three dihedral angles, such as rotational angle 1: 1-2-3-4, rotational angle 2: 5-1-2-3, and rotational angle 3: 2-3-4-10, exist for the neutral state of ethylene glycol with two hydroxyl groups. Three stable conformers, **3-D**, **3-E** and **3-F** were identified, when the neutral ethylene glycol was rotated around O-C-C-O (rotational angle 1) as shown in Fig. 8. **3-E** and **3-F** possess minimum energy and then **3-D** stabilizes at an energy level 1.57 kcal•mol<sup>-1</sup> higher than the others. In the cases of **3-E** and **3-F**, the hydroxyl groups face each other and formation of hydrogen bond is possible. On the other hand, the

Fig. 7 The fingerprint of HOMO energies for the monoanion derived from ethylene glycol.



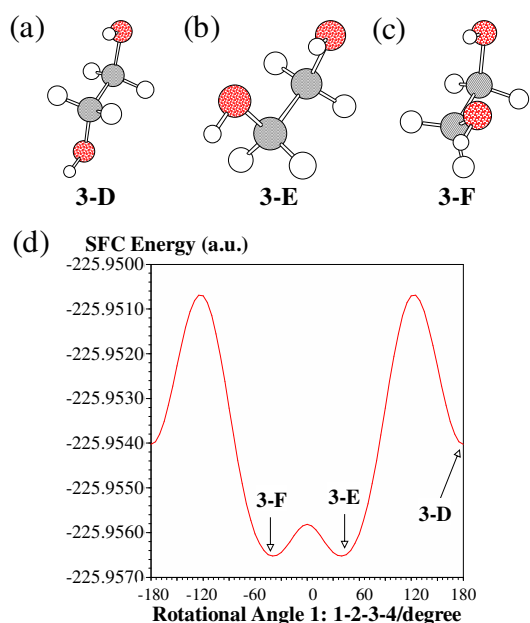


**Fig. 8** Stable conformers (a) 3-D, (b) 3-E and (c) 3-F obtained from the relative SCF and HOMO energy surfaces. (d) The relative SCF energy curve for ethylene glycol molecule rotated around O-C-C-O (rotational angle 1).

hydroxyl groups in **3-D** are farther away from each other, and the formation of the hydrogen bond that contributes to the stability of conformers is not realized.

Next, the relative surface energies and HOMO energies of the above three conformers were examined by rotating the two dihedral angles H-O-C-C (rotational angle 2: 5-1-2-3) and H-O-C-C (rotational angle 3: 2-3-4-10), while fixing the dihedral O-C-C-O (rotational angle 1). **3-E** and **3-F** behave similarly when the symmetry is taken into consideration. However, the calculations of all three conformers were carried out to prevent count loss.

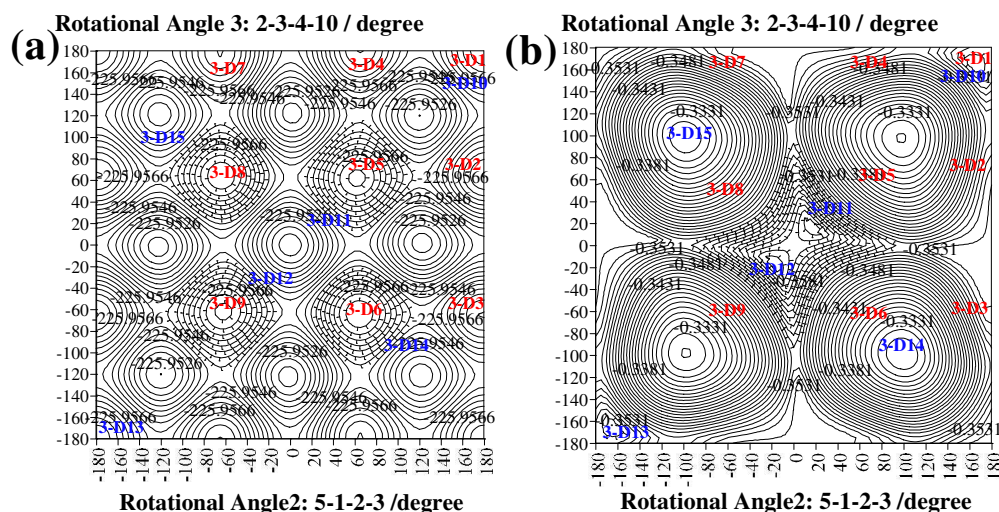
**Case (a): 3-D as the starting conformer.** When 3-D is considered as the starting structure, apparently 13 stable and characteristic conformers (Fig. S3), 9 from SCF energy surface

and 4 from HOMO energy surface, are obtained as shown in Fig. 9 (a) and (b) (enlarged version is shown in Fig. S4). When the duplication based on the symmetry is taken into account, the number of conformers is reduced to **3-D1** (180 (angle 1), 180 (angle 2)), **3-D2** (180,65), **3-D3** (180,-65), **3-D5** (60,60), **3-D6** (65,-65), **3-D10** (165,165), **3-D14** (100,-100) and **3-D15** (-100,100). But, considering the location of **3-D10** in the SCF energy surface (located in the slope and not in the stationary point), it was assumed unstable. Even though the orbital energy of **3-D14** (100,-100) and **3-D15** (-100,100), is -0.32925 a.u. and maximum among HOMO energies, they could be considered unstable since they are located in the slope and not in the stationary region. Consequently, the stable conformers obtained using **3-D** are reduced to five as shown in Fig. 10.

**Case (b): 3-E as the starting structure.** Similarly, when **3-E** is considered as the starting structure, apparently 18 stable and characteristic conformers, 9 from SCF energy surface and 9 from HOMO orbital energy surface are obtained (Fig. S5). The SCF and HOMO orbital energy surfaces for neutral state ethylene glycol in the case where 3-E as the starting structure is shown in Fig. S6. When the duplication based on the symmetry is taken into account, the number of conformers is reduced to **3-E1** (180 (angle 1),180 (angle 2)), **3-E2** (180,55), **3-E4** (55,55), **3-E5** (75,-30), **3-E7** (-40,-175), **3-E8** (-70,-70), **3-E10** (180,50), **3-E11** (165,-155), **3-E12** (15,180) and **3-E18** (105,105). Taking the locations of **3-E11** (165,-155) and **3-E12** (15,180) into account, they are considered unstable. Though **3-E18** has the maximum HOMO energy of -0.32517 a.u., it is not located in the stationary region. Thus it is also considered unstable. Similar results were obtained when **3-F** was used as the starting structure. The related data are given in Fig. S7 and S8.

The fingerprint in Fig. 11 describes the HOMO orbital energies of conformers obtained from the SCF and the HOMO orbital energy surfaces. Though the neutral state assumed some values, the range of HOMO energies was very narrow compared to the monoanion state.

**Fig. 9** (a) SCF and (b) HOMO orbital energy surfaces for neutral state ethylene glycol.



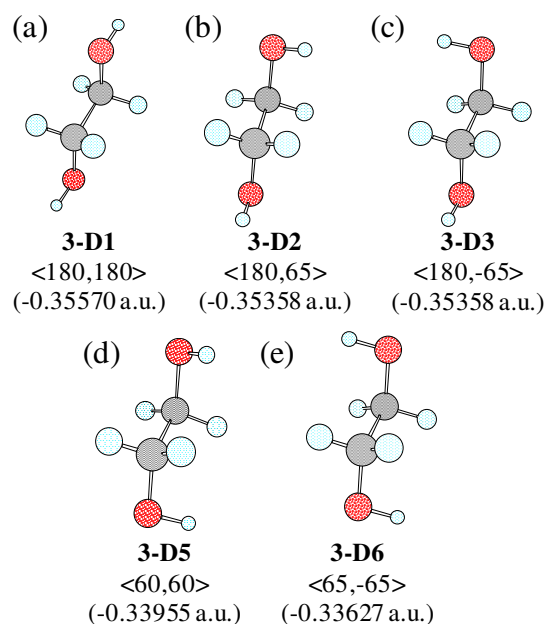


Fig. 10 Stable conformers obtained using 3-D as starting structure.

The HOMO energies of the neutral, monoanion and dianion states of ethylene glycol are shown in Fig. 12. The HOMO energy level increases in the order of neutral, monoanion and dianion states. The reaction rates of monoanion and dianion states are higher than that of the neutral state. Considering the actual experimental conditions and the mass balance between ethylene glycol and sodium hydroxide, it is very difficult to assume that the dianion state of ethylene glycol could exist. The probability of the presence of dianion is assumed extremely low. On the other hand, though the reactivity of ethylene glycol itself is very poor or very slow, the introduction of sodium hydroxide induces the formation of the monoanion and the rapid progression of the reaction could be expected. The orbital energy in the monoanion state is reasonably high even in the absence of heating. However, when heated, the energy

Fig. 11 The finger print of HOMO energies for neutral ethylene glycol species.

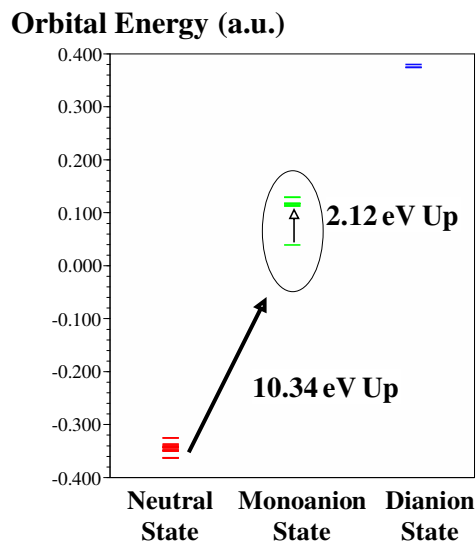
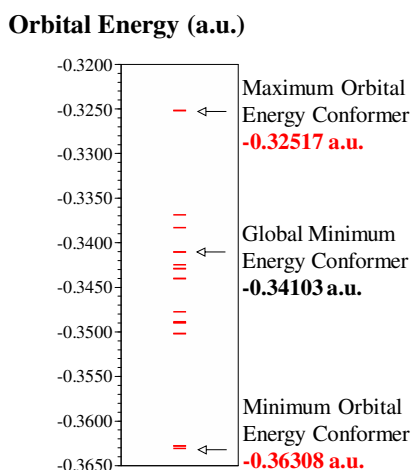


Fig. 12 HOMO energies of the neutral, monoanion and dianion states of ethylene glycol.

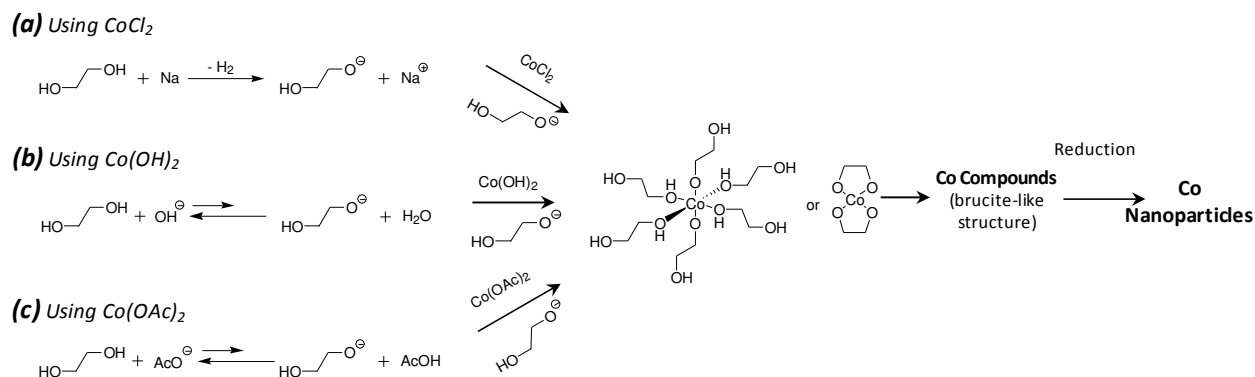
increases further by 2.12 eV and ethylene glycol becomes more reactive. The orbital energy of the monoanion state of ethylene glycol is higher than that of the neutral state. Thus, the theoretical calculations predict that the monoanion state of ethylene glycol acts as the true active species under normal experimental conditions.

In the next section, we report the results of the experiments carried out to verify the theoretical prediction and also look into the possibilities of explaining some unresolved issues in the synthesis of metal particles by polyol process using ethylene glycol as solvent with different metal salts.

### Experimental verification of theoretical predictions

Synthesis of cobalt metal particles using polyol process has been well established in the middle of 1980's.<sup>47,56-60</sup> The use of sodium hydroxide as an additive to accelerate the reaction is also being practiced in synthesizing various metals using polyol process,<sup>37,61-68</sup> but no convincing explanation has been provided. Furthermore, in most cases, cobalt acetate has been used as the metal source,<sup>47,69-73</sup> even though cobalt chloride or other cobalt salts were readily available. But, nothing has been stated for the selection of cobalt acetate among the salts available. Plausible explanation for the above experimental practice is attempted in the light of the theoretical prediction, which suggests that the true active species is the monoanion state of ethylene glycol.

**Case (a): Synthesis of metallic cobalt particles using cobalt chloride as metal precursor.** Formation of different metallic compounds in polyols is preceded by the dissolution of the precursor salt. Crystalline materials are obtained in ethylene glycol and the structural resolutions clearly showed that monoanion state of polyol complex with the metal cations to form glycoxide species.<sup>74,75</sup>



**Scheme 1** The reaction scheme for the synthesis of cobalt metal particles using different cobalt precursors in ethylene glycol.

To test the hypothesis, initially, the synthesis of cobalt metal particles using cobalt chloride in ethylene glycol was attempted. Though the cobalt chloride dissolved in ethylene glycol, the solution changed its color from pink (at R.T) to blue and no visible precipitate was obtained even the solution was heated to the boiling point of ethylene glycol and refluxed at this temperature for more than 24 hours. Based on the conclusion derived from the theoretical calculations, the inability to generate monoanion state of ethylene glycol and subsequent formation of cobalt ethylene glycoxide may have prevented the progress of the reaction.

Thus, to confirm the formation of metallic cobalt through cobalt glycoxide route, sodium glycoxide was synthesized by reacting equimolar ethylene glycol and sodium metal in dodecane. Sodium metal was preferred over sodium hydroxide to prevent the formation of cobalt hydroxide in the subsequent step. This resulted in the formation of a white precipitate, presumably sodium glycoxide according to the reaction shown in Scheme 1(a). Then, the white precipitate was reacted with cobalt chloride anhydrous in dodecane to form cobalt glycoxide. The XRD pattern of this precipitate resulted to be similar to what was reported by Chakroune et al.<sup>72</sup> and is shown in Fig. S9(a). Then, the cobalt glycoxide thus prepared was heated in dodecane, to confirm that subsequent electron transfer is necessary for the formation of metal cobalt. As expected, no visible change was observed. Thus, the cobalt glycoxide prepared using the above technique was introduced in ethylene glycol and heated to the boiling point under nitrogen purging. Consequently, a black magnetic precipitate with a saturation magnetization of 160 emu/g was obtained. Here, the reaction is assumed to have progressed according to Scheme 1(a). The structural analysis of the black magnetic precipitate confirmed presence of metallic cobalt composed of fcc and hcp crystal structures (Fig. S10). These results confirmed that cobalt glycoxide was the active complex, which was subsequently reduced by ethylene glycol to form Co metal particles. However, it should be noted that the particles were submicrometer sized aggregate composed of particles of few tens of nanometer in diameter from the SEM measurements (Fig. S11(a)). This confirmed that the alkoxide route is very effective for the reduction of metal ions by polyol.

But, it should be noted that in contrast to the cobalt chloride case, the formation metallic cobalt has been observed in the case where cobalt acetate was used as metal precursor. This disparity has not been explained or discussed until now. In the light of the present theoretical finding, we have attempted to explain the difference in the easiness with which the cobalt metal particles are formed for different types of metal salts such as cobalt hydroxide and cobalt acetate.

**Case (b): Synthesis of metallic cobalt particles using cobalt hydroxide as metal precursor.** Next, the synthesis of metallic cobalt was attempted using cobalt hydroxide as the metal precursor. Cobalt hydroxide was prepared by reacting cobalt chloride with sodium hydroxide in water and the pink colored precipitate thus obtained was washed with water and acetone and introduced into ethylene glycol. The cobalt hydroxide changed to brucite-like precipitated as the cobalt hydroxide - ethylene glycol system was heated to 190 °C. However, when the system was heated for more than 1 hour, the reduction reaction progressed and the solid substance dispersed in ethylene glycol turned black. Though the synthesis of cobalt metal particles required prolonged heating, the formation of metallic cobalt was confirmed from the XRD and magnetic measurements. We believe that the hydroxyl ion was replaced with ethylene glycol monoanion to form the intermediate pink colored cobalt alkoxide precipitate prior to subsequent reduction of the same to precipitate metallic cobalt (Fig. S10(b)). We believe that the replacement of the hydroxyl ion by the monoanion state of ethylene glycol in the brucite-like structured cobalt hydroxide was the rate determining reaction. The hydroxyl ion thus excreted from the cobalt hydroxide deprotonated the ethylene glycol to give rise to monoanion state molecules, which subsequently formed cobalt ethylene glycoxide as confirmed by XRD analysis (Fig. S9(b)). As proposed by the theoretical estimation, the formation of the active species, monoanion of ethylene glycol, is necessary for the dissolution and reduction of cobalt species. The prolonged heating of cobalt hydroxide in ethylene glycol facilitates the excretion of hydroxyl ion. Scheme 1(b) shows the possible reaction schemes for the dissolution and reduction of cobalt species in ethylene glycol. We believe that the deprotonating

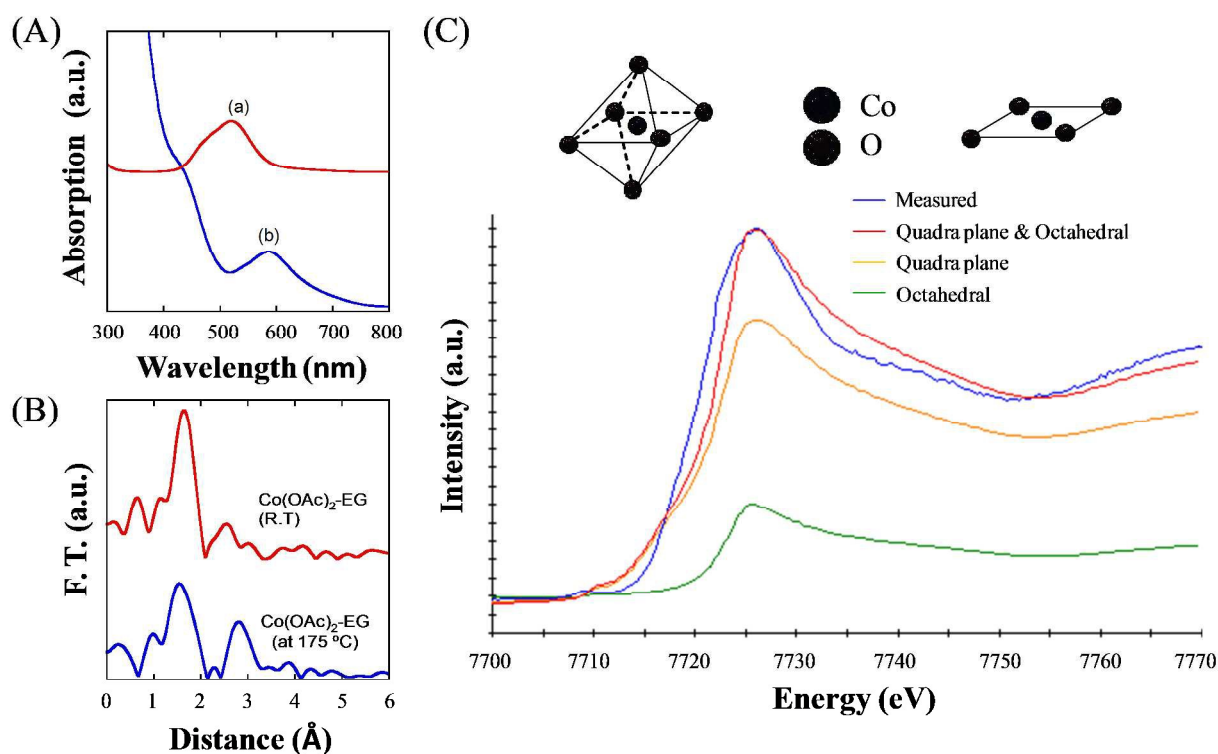


**Fig. 13** (A) UV-vis spectra of Co(OAc)<sub>2</sub>-EG at (a) R.T and (b) 175 °C. (B) Fourier transformed profiles of Co(OAc)<sub>2</sub>-EG solutions at (a) R.T. and (b) 175 °C. (C) FEFF fitting of the profiles using tetra- and hexa-coordinated structural configurations

ability of hydroxyl ion is greater than chloride ion in addition to the difference in dissociation constants of cobalt chloride and cobalt hydroxide.<sup>76</sup>

As already stated before, the formation of metallic cobalt was not realized when cobalt chloride was used as metal precursor. We believe that the result is a consequence of the fact that the dissociation of cobalt chloride in ethylene glycol and subsequent reaction of chloride ion with ethylene glycol to deprotonate the same to form the monoanion state of ethylene glycol was not realized. However, when metal Na or NaOH were used, though initially considered as accelerator of the reaction or pH modifier, these eased the deprotonation reaction of ethylene glycol forming cobalt ethylene glycoxide which is more reducible than CoCl<sub>2</sub> according to the scheme 1(a) and (b).

**Case (c): Synthesis of metallic cobalt particles using cobalt acetate as metal precursor.** Finally, let us consider the case of cobalt acetate as the metallic precursor. When cobalt acetate was introduced into ethylene glycol and heated to the boiling point, the precipitation of metallic cobalt was observed even in the absence of either sodium hydroxide or sodium metal. Furthermore, the formation of the cobalt alkoxide and their subsequent reduction to metallic cobalt (Fig. S10(c)) was realized in comparatively shorter reaction time than in the cases of other metallic precursors. Here, the cobalt acetate - ethylene glycol mixture turned to green in color from pink when the system was heated to higher temperature. Further heating gave

rise to the formation of pink colored precipitate, which subsequently turned to black. The coordination chemistry of metal ions with ethylene glycol is relevant in understanding the reaction kinetics and solvent and ion exchange during complex formation and subsequent reduction reactions.

Several groups have attempted to elucidate the reaction mechanism in polyol process<sup>77-80</sup> and postulated the formation of metal glycoxide as possible intermediates. However, the definite structural details of these intermediates have not been reported. Recently, the structural details of a Cu<sup>2+</sup> glycolate obtained from ethylene glycol - copper chloride dehydrate - sodium hydroxide system has been experimentally investigated and the presence of an anionic moiety consisting bis-ethylene glycolate Cu<sup>2+</sup> dianion<sup>81</sup> has been confirmed. However, in the present system, sodium hydroxide has not been used and also the cobalt salt considered is not chloride, but acetate. However, still the formation of cobalt complexes prior the precipitation of cobalt glycoxide has been observed. To understand the changes taking place during the reduction reaction, samples were taken at different temperatures and their structures were evaluated using UV-Vis and EXAFS. The results are shown in Fig. 13. The results of UV-vis spectroscopic measurements of the cobalt complex at (a) R.T and (b) 175 °C are shown in Fig. 13(A). In the case of the sample obtained at low temperature, the appearance of two peaks at 489 and 520 nm were confirmed. From the previous literature, it is inferred that the complex has octahedral coordination.<sup>82</sup> On the other hand, in the case of the sample obtained at higher temperature; the appearance of a

peak at 575 nm was recorded. This inferred the formation of tetrahedral coordination.<sup>83</sup> When cobalt acetate is heated in excess ethylene glycol, the glycol loses its two protons and the dianion complexes the metal center to give a compound whose metal to ethylene glycol ratio is almost two.<sup>84</sup>

To confirm the structural details, the samples were analyzed using EXAFS at Co-K-edge. The Fourier-transformed profiles of the samples obtained at (a) low and (b) high temperatures are shown in Fig. 13(B). The co-ordination number and the Co-O bond length obtained by analyzing the first nearest peak that corresponds to oxygen was determined to be 6 and 2.07 Å for the sample obtained at low temperature and 4 and 2.04 Å for the sample obtained at higher temperature. Furthermore, the presence of a strong peak at higher distance from Co atom was observed only for the sample obtained at higher temperature. When the second nearest neighbour peak was fitted assuming that it originated from Co-Co correlation, the bond length was estimated to be about 3 Å. However, obtaining a reliable value for the coordination number was considered difficult. Furthermore, the structural details of the pink precipitate obtained prior to the formation of metallic cobalt were also analyzed using EXAFS.

To our surprise, the profile was very similar to the liquid sample obtained at higher temperature. The cobalt glycoxide has been reported to present a layered structure de-rived from the brucite-like structure with turbostratic disorder along the c-axis. In the brucite-like structured cobalt ethylene glycoxide, the Co - Co distance deduced roughly from the (100) and (110) positions, is determined to be 3.09 Å,<sup>85</sup> and matches well with the distance obtained from the fitting of the second nearest neighbor peak corresponding to Co-Co distance in the sample obtained at higher temperature. The validity of prospective models was evaluated by fitting the XANES profile using FEFF (Fig. 13(C)). First, the FEFF analysis was carried out for the sample obtained at low temperature assuming octahedral coordination.

The measured and the calculated profiles matched well and confirmed the validity of the assumption. Secondly, based on the EXAFS profile obtained for the sample at higher temperature, fitting of different tetrahedral coordinated configurations were attempted. Among the considered configurations, the matching between measured and observed spectra of quadra plane coordination of oxygen atoms with cobalt was comparatively good. However, portion of the spectrum (higher energy region) doesn't fit well and the possibility of having a mixture of both tetrahedral and octahedral coordinated complexes was examined. Careful observation of the XANES profiles of both complexes, the miss fit area of the calculated profile for the sample obtained at higher temperature has the features corresponding to the complex obtained at lower temperature. Thus, calculations using various ratios of tetrahedral- and octahedral-coordinated complexes were performed. As a consequence, the fitting improved and the sample obtained at higher temperature was assumed to contain 75 of tetrahedral coordinated and 25 % of octahedral coordinated complexes as shown in Fig. 13(C).

Here again, the results can be explained based on the relative easiness with which the formation of monoanion state of ethylene glycol is realized. We believe that the formation of ethylene glycol anion is achieved through the deprotonation reaction by the acetate ion, generated through the dissociation of cobalt acetate, and ethylene glycol. However, recent studies suggested that the complex formation of divalent metal ions is possible even in the absence of deprotonation of the diol. Complex formation of divalent metal anions with diols, in the presence of anion auxiliary ligands has been studied recently by Ruttink et al.<sup>86</sup> Ternary complexes of the type AH(diol)...Co<sup>2+</sup>...CH<sub>3</sub>COO<sup>-</sup>(ligand) in the gas phase has been identified using MALDI (Matrix Assisted Laser Desorption/Ionization) and ESI(Electron Spray Ionization), and their dissociation characteristics have been obtained. They reported that the auxiliary ligands such as acetate ion enable the complex formation with diol such as ethylene glycol without ethylene glycol becoming deprotonated. Thus, the formation of acetic acid is also possible from admixture of HOCH<sub>2</sub>CH<sub>2</sub>OH...Co<sup>2+</sup>...-OOCCH<sub>3</sub>. This promotes the formation of cobalt ethylene glycoxide and their subsequent reduction to generate metallic cobalt. The possible reaction schemes for the dissolution and reduction of cobalt species in ethylene glycol using cobalt acetate as the metallic precursor is described in Scheme 1(c). The dissociation constants of cobalt acetate and acetic acid may also be a key for reaction kinetics of the overall reaction.

## Conclusions

The synthesis of metal particles by polyol process using any metal salt precursor has been made possible. Though the scheme for synthesis of cobalt metal particles using any metal precursor has been established, the particles were agglomerated and sub-micrometer in size. This was considered due to the morphology of the cobalt intermediate formed prior to the reduction reaction. Thus, for the synthesis of monodispersed metallic cobalt nanoparticles reaction scheme that evades the formation of brucite-like structured intermediate should be designed. The research is in progress aiming at understanding the overall reaction taking place on the polyol side (oxidation) as well as in the metal side (reduction) for designed metal and alloy nanoparticle synthesis.

## Acknowledgements

This work was supported by Grant-in Aid for Basic Research #(B) 22310064 and Challenging Exploratory Research 25600028 from Ministry of Education, Culture, Sports, Science, and Technology of Japan (MEXT), Japan.

## Notes and references

<sup>a</sup> Institute of Multidisciplinary Research for Advanced Materials, Tohoku University, Sendai, 980-8577, Japan. Fax: 81 22 217 5108; Tel: 8122 217 5108; E-mail: matsu@tagen.tohoku.ac.jp.

<sup>b</sup> Department of Material Science, The University of Shiga Prefecture, Hikone 522-8533, Japan. Fax: 81 749 28 8486; Tel: 81 749 28 8352; E-mail: jeyadevan.b@mat.usp.ac.jp

<sup>a</sup> ITODYS, University of Diderot, Paris, France. Fax: 33 1 57 27 68 68; Tel: 33 1 57 27 72 63; E-mail: [jean-yves.piquemal@paris7.jussieu.fr](mailto:jean-yves.piquemal@paris7.jussieu.fr).

† Electronic Supplementary Information (ESI) available: Structures obtained from SCF and HOMO energy surfaces of ethylene glycol at each state (S1~S8), the X-ray diffraction patterns and SEM photographs of Co compounds (S9~S11). See DOI: 10.1039/b000000x/

- 1 K. Na, Q. Zhang, G. A. Somorjai, *J. Clust. Sci.*, 2014, **25**, 83-114.
- 2 Y. Sun, *Chem. Soc. Rev.*, 2013, **42**, 2497-2511.
- 3 S. Chaturvedi, P. N. Dave, *J. Mater. Sci.*, 2013, **48**, 3605-3622.
- 4 M. B. Cortie, A. M. McDonagh, *Chem. Rev.*, 2011, **111**, 3713-3735.
- 5 A. K. Sra, T. D. Ewers, R. E. Schaak, *Chem. Mater.*, 2005, **17**, 758-766.
- 6 A. G. Boudjahem, S. Monteverdi, M. Mercy, M. M. Bettahar, *J. Catalysis*, 2004, **221**, 325-334.
- 7 S. Hokenek, C. Bennett, J. N. Kuhn, *J. Cryst. Growth*, 2013, **374**, 18-22.
- 8 T. Matsushita, T. Iwamoto, M. Inokuchi, N. Toshima, *Nanotechnology*, 2010, **21**, 095603.
- 9 C. X. Kan, C. S. Wang, H. C. Li, J. S. Qi, J. J. Zhu, Z. S. Li, D. N. Shi, *Small*, 2010, **6**, 1768-1775.
- 10 J. Jin, K. Suganuma, M. Nogi, *J. Mater. Sci.*, 2011, **46**, 4964-4970.
- 11 N. S. Bell, D. R. Tallant, *J. Sol-Gel Sci. Tech.*, 2009, **51**, 158-168.
- 12 I. S. Lyubutin, S. S. Starchikov, C. -R. Lin, S. -Z. Lu, M. O. Shaikh, K. O. Funtov, T. V. Dmitrieva, S. G. Ovchinnikov, I. S. Edelman, R. Ivantsov, *J. Nanopart. Res.*, 2013, **15**, 1397.
- 13 N. L. Henderson, M. D. Straesser, P.E. Sabato, R. E. Schaak, *Green Chem.*, 2009, **11**, 974-978.
- 14 A. Datta, D. Mukherjee, S. Witanachchi, P. Mukherjee, *RSC Advances*, 2013, **3**, 141-147.
- 15 M. Blosi, S. Albonetti, S. Ortelli, A. L. Costa, L. Ortolani, M. Dondi, *New J. Chem.*, 2014, **38**, 1401-1409.
- 16 T. Parnklang, C. Lertvachirapaiboon, P. Pienpinijtham, K. Wongravee, C. Thammacharoen, S. Ekgasit, *RSC Advances*, 2013, **3**, 12886-12894.
- 17 P. P. Shanbogh, S. C. Peter, *RSC Advances*, 2013, **3**, 22887-22890.
- 18 D. Wang, Q. Wang, T. Wang, 2010, **12**, 3797-3805.
- 19 R. E. Cable, R. E. Schaak, *Chem. Mater.*, 2005, **17**, 6835-6841.
- 20 M. Vondrova, C. M. Burgess, A. B. Bocarsly, *Chem. Mater.*, 2007, **19**, 2203-2212.
- 21 H. T. Zhang, J. Ding, G. M. Chow, M. Ran, J. B. Yi, *Chem. Mater.*, 2009, **21**, 5222-5228.
- 22 S. L. Gai, C. X. Li, P. P. Yang, J. Lin, *Chem. Rev.*, 2014, **114**, 2343-2389.
- 23 N. Miguel-Sancho, O. Bomati-Miguel, A. G. Roca, G. Martinez, M. Arruebo, J. Santamaria, *Ind. Eng. Chem. Res.*, 2012, **51**, 8348-8357.
- 24 M. C. Liu, Y. Q. Zheng, L. Zhang, L. J. Guo, Y. N. Xia, *J. Am. Chem. Soc.*, 2013, **135**, 11752-11755.
- 25 Y. M. Chen, F. Yang, Y. Dai, W. Q. Wang, S. L. Chen, *J. Phys. Chem. C*, 2008, **112**, 1645-1649.
- 26 A. Anžlovar, Z. C. Oreš, M. Žigon, *J. Nanosci. Nanotech.*, 2008, **8**, 3516-3525.
- 27 J. H. Kou, C. Bennett-Stamper, R. S. Varma, *ACS Sustainable Chem. Eng.*, 2013, **1**, 810-816.
- 28 M. H. Khedr, A. A. Farghali, A. A. Abdel-Khalek, *J. Anal. Appl. Pyrolysis*, 2007, **78**, 1-6.
- 29 K. Morita, G. Mera, K. Yoshida, Y. Ikuhara, A. Klein, H. J. Kleebe, R. Riedel, *Solid State Sci.*, 2013, **23**, 50-57.
- 30 P. Hermankova, M. Hermanek, R. Zboril, *Eur. J. Inorg. Chem.*, 2010, 1110-1118.
- 31 G. X. Tong, J. G. Guan, Q. J. Zhang, *Adv. Funct. Mater.*, 2013, **23**, 2406-2414.
- 32 P. A. Chernavskii, P. V. Afanas'ev, G. V. Pankina, N. S. Perov, *Russ. J. Phys. Chem. A*, 2008, **82**, 2176-2181.
- 33 M. M. Walz, F. Vollnhals, M. Schirmer, H. P. Steinrück, H. Marbach, *Phys. Chem. Chem. Phys.*, 2011, **13**, 17333-17338.
- 34 C. Y. Lin, Y. H. Lai, D. Mersch, E. Reisner, *Chem. Sci.*, 2012, **3**, 3482-3487.
- 35 K. V. Manukyan, A. Cross, S. Roslyakov, S. Rouvimov, A. S. Rogachev, E. E. Wolf, A. S. Mukasyan, *J. Phys. Chem. C*, 2013, **117**, 24417-24427.
- 36 R. Banerjee, P. A. Crozier, *J. Phys. Chem. C*, 2012, **116**, 11486-11495.
- 37 R. J. Joseyphus, K. Shinoda, D. Kodama, B. Jeyadevan, *Mater. Chem. Phys.*, 2010, **123**, 487-493.
- 38 R. J. Joseyphus, D. Kodama, T. Matsumoto, Y. Sato, B. Jeyadevan, K. Tohji, *J. Magn. Magn. Mater.*, 2007, **310**, 2393-2395.
- 39 D. Kodama, K. Shinoda, K. Sato, Y. Sato, B. Jeyadevan, K. Tohji, *J. Magn. Magn. Mater.*, 2007, **310**, 2396-2398.
- 40 S. Sun, *Adv. Mater.*, 2006, **18**, 393-403.
- 41 D. Kodama, K. Shinoda, K. Sato, Y. Konno, R. J. Joseyphus, K. Motomiya, H. Takahashi, T. Matsumoto, Y. Sato, K. Tohji, B. Jeyadevan, *Adv. Mater.*, 2006, **18**, 3154-3159.
- 42 R. J. Joseyphus, K. Shinoda, Y. Sato, K. Tohji, B. Jeyadevan, *J. Mater. Sci.*, 2008, **43**, 2402-2406.
- 43 M. B. Cortie, A. M. McDonagh, *Chem. Rev.*, 2011, **111**, 3713-3735.
- 44 J. L. C. Huaman, K. Sato, S. Kurita, T. Matsumoto and B. Jeyadevan, *J. Mater. Chem.*, 2011, **21**, 7062-7069.
- 45 J. L. C. Huaman, N. Hironaka, S. Tanaka, K. Shinoda, H. Miyamura, B. Jeyadevan, *CrystEngComm*, 2013, **15**, 729-737.
- 46 J. L. C. Huaman, S. Fukao, K. Shinoda, B. Jeyadevan, *CrystEngComm*, 2011, **13**, 3364-3369.
- 47 R. J. Joseyphus, T. Matsumoto, H. Takahashi, D. Kodama, K. Tohji, B. Jeyadevan, *J. Solid State Chem.*, 2007, **180**, 3008-3018.
- 48 J. Y. Piquemal, G. Viau, P. Beaunier, F. Bozon-Verduraz, F. Fiévet, *Mater. Res. Bull.*, 2003, **38**, 389-394.
- 49 K. J. Carroll, J. U. Reveles, M. D. Shultz, S. N. Khanna, E. E. Carpenter, *J. Phys. Chem. C*, 2011, **115**, 2656-2664.
- 50 Gaussian 98, Revision A.11.3: M. J. Frisch, G. W. Trucks, H. B. Schlegel, G. E. Scuseria, M. A. Robb, J. R. Cheeseman, V. G. Zakrzewski, J. A. Montgomery, Jr., R. E. Stratmann, J. C. Burant, S. Dapprich, J. M. Millam, A. D. Daniels, K. N. Kudin, M. C. Strain, O. Farkas, J. Tomasi, V. Barone, M. Cossi, R. Cammi, B. Mennucci, C. Pomelli, C. Adamo, S. Clifford, J. Ochterski, G. A. Petersson, P. Y. Ayala, Q. Cui, K. Morokuma, N. Rega, P. Salvador, J. J. Dannenberg, D. K. Malick, A. D. Rabuck, K. Raghavachari, J. B. Foresman, J. Cioslowski, J. V. Ortiz, A. G. Baboul, B. B. Stefanov, G. Liu, A. Liashenko, P. Piskorz, I. Komaromi, R. Gomperts, R. L. Martin, D. J. Fox, T. Keith, M. A. Al-Laham, C. Y. Peng, A. Nanayakkara, M. Challacombe, P. M. W. Gill, B. Johnson, W. Chen,

- M. W. Wong, J. L. Andres, C. Gonzalez, M. Head-Gordon, E. S. Replogle, and J. A. Pople, Gaussian, Inc., Pittsburgh PA, 2002.
- 51 W. J. Hehre, R. F. Stewart and J. A. Pople, *J. Chem. Phys.*, 1969, **51**, 2657-2664.
- 52 J. B. Collins, P. v. R. Schleyer, J. S. Binkley, J. A. Pople, *J. Chem. Phys.*, 1976, **64**, 5142-5151.
- 53 P. J. Hay, W. R. Wadt, *J. Chem. Phys.*, 1985, **82**, 270-283
- 54 W. R. Wadt, P. J. Hay, *J. Chem. Phys.*, 1985, **82**, 284-298.
- 55 P. J. Hay, W. R. Wadt, *J. Chem. Phys.*, 1985, **82**, 299-310.
- 56 M. Figlarz, F. Fiévet, J. P. Lagier, French Patent No. 82 21483 (Dec. 21, 1982), Europe Patent No. 0113281 (Dec. 20, 1983), U.S. Patent No. 4539041, Finland Patent No. 74416. Japan Application No. 24303783.
- 57 F. Fievet, J. P. Lagier and M. Figlarz, *MRS Bull.*, 1989, 29-34.
- 58 F. Fievet, J. P. Lagier, B. Blin, B. Beaudoin, M. Figlarz, *Solid States Ionics*, 1989, **32/33**, 198-205.
- 59 O. Perales-Perez, B. Jeyadevan, C. N. Chinnasamy, K. Tohji, A. Kasuya, *IPAP Conf. Series 3*, 2001, 105-108.
- 60 O. Perales-Perez, B. Jeyadevan, C. N. Chinnasamy, K. Tohji, A. Kasuya, Synthesis of structure and size controlled Co nanoparticles and their magnetic properties, Inorganic Materials: Recent Advances, Narosa Publishing House, Mumbai, India, 2004; pp 9-15.
- 61 S. Fujieda, K. Shinoda, S. Suzuki, B. Jeyadevan, *IEEE Transactions on Magnetics*, 2013, **49**, 3303-3306.
- 62 R. J. Joseyphus, B. Jeyadevan, *J. Phys. Chem. Solids*, 2011, **72**, 1212-1217.
- 63 B. Jeyadevan, C. N. Chinnasamy, O. Perales-Perez, Y. Iwasaki, A. Hobo, K. Shinoda, K. Tohji, A. Kasuya, *IEEE Transactions on Magnetics*, 2002, **38**, 2595-2597.
- 64 B. Jeyadevan, K. Urakawa, A. Hobo, N. Chinnasamy, K. Shinoda, K. Tohji, D. D. J. Djayaprawira, M. Tsunoda, M. Takahashi, *Jpn. J. Appl. Phys.*, 2003, **42**, L350-L352.
- 65 C. N. Chinnasamy, B. Jeyadevan, K. Shinoda and K. Tohji, *J. Appl. Phys.*, 2003, **93**, 7583-7585
- 66 H. Yin, G. M. Chow, *J. Electrochem. Soc.*, 2002, **149**, C68-C73.
- 67 K. K. Caswell, C. M. Bender, C. J. Murphy, *Nano Lett.*, 2003, **3**, 667-669.
- 68 E. Hosono, S. Fujihara, T. Kimura, H. Imai, *J. Sol-Gel Sci. Tech.*, 2004, **29**, 71-79.
- 69 C. Osorio-Cantillo, A. N. Santiago-Miranda, O. Perales-Perez, Y. Xin, Y., *J. Appl. Phys.*, 2012, **111**, 07B324.
- 70 W. T. Cheng, H. W. Cheng, *AIChE J.*, 2009, **55**, 1383-1389.
- 71 R. Vasanthi, D. Kalpana, N. G. Renganathan, *J. Solid State Electrochem.*, 2008, **12**, 961-969.
- 72 N. Chakroune, G. Viau, S. Ammar, N. Jouini, P. Gredin, M. J. Vaulay, F. Fievet, *New. J. Chem.*, 2005, **29**, 355-361.
- 73 N. Chakroune, G. Viau, C. Ricolleau, F. Fiévet-Vincent, F. Fiévet, *J. Mater. Chem.*, 2003, **13**, 312-318.
- 74 L. Poul, N. Jouini, F. Fiévet, P. Herson, *Z. Kristallogr.*, 1998, **213**, 416-418.
- 75 N. Jouini, L. Poul, F. Fiévet, F. Robert, *Eur. J. Solid State Inorg. Chem.*, 1995, **32**, 1129-1136.
- 76 D. R. Lide, editor-in-chief., CRC handbook of chemistry and physics 89th Edition, CRC Press, Inc., Boca Raton, Florida, 2008.
- 77 F. Bonet, K. Tekaiia-Elhsissen, K. V. Sarathy, *Bull. Mater. Sci.*, 2000, **23**, 165-168.
- 78 F. Fievet, J. P. Lagier, B. Beaudoin, M. Figlarz, *Solid States Ionics*, 1988, **26**, 154-154.
- 79 A. Pasquarello, I. Petri, P. S. Salmon, O. Parisel, R. Car, É. Tóth, D. H. Powell, H. E. Fischer, L. Helm, A. E. Merbach, *Science*, 2001, **291**, 856-859.
- 80 P. S. Salmon, P. B. Lond, *J. Phys. Condens. Mater.*, 1992, **4**, 5249-5262.
- 81 J. H. Rivers, K. J. Carroll, R. A. Jones, E. E. Carpenter, *Acta Cryst.*, 2010, **C66**, m83-m85.
- 82 A. B. P. Lever, Inorganic Electronic Spectroscopy, Elsevier, Amsterdam, 1968.
- 83 L. I. Katzin, E. Gebert, *J. Am. Chem. Soc.*, 1950, **72**, 5464-5471.
- 84 N. Chakroune, G. Viau, S. Ammar, N. Jouini, P. Gredin, M. J. Vaulay, F. Fiévet, *New. J. Chem.*, 2005, **29**, 355-366.
- 85 F. A. Cotton, R. C. Elder, *Inorg. Chem.*, 1965, **4**, 1145-1151.
- 86 P. J. A. Ruttink, L. J. M. Dekker, T. M. Luider, P. C. Burgers, *J. Mass. Spectrom.*, 2012, **47**, 869-874.